IMMUNOPATHOLOGY AND INFECTIOUS DISEASES

Penetration of CD8+ Cytotoxic T Cells into Large Target, Tissue Cysts of *Toxoplasma gondii*, Leads to Its Elimination

Check for updates

Ashish Tiwari,* Rancie Hannah,* Jenny Lutshumba,* Eri Ochiai,* Louis M. Weiss,[†‡] and Yasuhiro Suzuki*[§]

From the Department of Microbiology, Immunology and Molecular Genetics, University of Kentucky College of Medicine, Lexington, Kentucky; the Departments of Pathology[†] and Medicine,[‡] Albert Einstein College of Medicine, Bronx, New York; and the Department of Biomedical Sciences and Pathobiology,[§] Virginia Polytechnic Institute and State University, Blacksburg, Virginia

CD8+ cytotoxic T cells kill target cells through direct cell-cell contact. However, it remains unclear how these T cells eliminate a target of large mass. We investigated how CD8+ T cells remove tissue cysts of *Toxoplasma gondii*, which can grow to the size of >50 μm in diameter within infected cells. Notably, immunohistologic analyses in the brains of infected mice visualized the presence of numbers of CD8+ immune T cells that had migrated halfway through the cyst wall as well as T cells located fully within the cysts. Perforin was required for their invasion and cyst elimination. Cysts invaded by the T cells displayed morphologic deterioration and destruction. Within these deteriorated cysts, granular structures intensely positive for granzyme B were detected in association with *T. gondii* bradyzoites. Furthermore, the bradyzoites within the destroyed cysts were located within accumulated ionized calcium binding adaptor molecule 1 (Iba1)-positive microglia and Ly6C+ macrophages, suggesting that these phagocytes had phagocytosed those organisms for their eradication. The present study uncovered a previously unappreciated capability of CD8+ cytotoxic T cells to penetrate into a large target, *T. gondii* cysts, for their elimination. This invasive capability of CD8+ cytotoxic T cells in collaboration with phagocytes appears to be a powerful effector mechanism that functions against not only *T. gondii* cysts but also other large targets, including solid cancers. *(Am J Pathol 2019, 189: 1594−1607; https://doi.org/10.1016/j.ajpath.2019.04.018)*

Toxoplasma gondii is an obligate intracellular protozoan parasite that can establish a chronic infection in humans. One-third of the human population in the world is estimated to be infected with this parasite.[1] The basis of the persistent chronic infection is the cysts, which can contain hundreds to thousands of bradyzoites surrounded by the cyst wall,[2−4] in various organs, especially the brain. This chronic infection can reactivate in immunocompromised individuals, such as those with AIDS, neoplastic diseases, and organ transplants, resulting in life-threatening toxoplasmic encephalitis.[1] Even in immunocompetent individuals, recent epidemiologic studies shed light on the pathogenic effects of this widespread chronic infection by reporting a higher incidence of multiple types of cancers in individuals seropositive to this parasite.[5−7] Current chemotherapy is effective only against tachyzoites. Therefore, there is an urgent need to develop

technique(s) capable of eradicating the cyst stage of *T. gondii* from chronically infected individuals. Therefore, development of an immunologic intervention capable of attacking and eradicating the cysts is a valuable approach to fight against this widespread infection.

Although information exists on the molecular mechanisms of the interferon (IFN)-γ−mediated protective immunity to control proliferation of *T. gondii* tachyzoites (the acute stage form),[8,9] the mechanisms of the host immunity against the cyst stage of the parasite are not well understood. Our recent studies revealed that an adoptive transfer of

CD8$^+$ immune T cells from chronically infected mice to infected immunodeficient [athymic nude or severe combined immunodeficiency (SCID)] animals, which have already established large numbers of cysts in their brains, is able to markedly reduce numbers of the cysts in the brains of the recipients.[10] Notably, in contrast to the protective immunity against tachyzoites, the capability of CD8$^+$ T cells to produce IFN-γ is dispensable for their activity to reduce the cyst numbers.[10] Of interest, perforin was found to be required for the activity of CD8$^+$ T cells to reduce cyst numbers in the brains of infected mice.[10] However, how CD8$^+$ T cells reduce *T. gondii* cyst burden using their perforin-mediated activity remains to be elucidated. In the present study, we determined that perforin-mediated cyst burden reduction is not due to indirect effects of inhibiting tachyzoite proliferation but is due to the direct removal of pre-existing cysts. Furthermore, immunohistochemical studies visualized that CD8$^+$ immune T cells are capable of invading into cysts during the anticyst immune process in the brains of infected mice. The T-cell—invaded cysts displayed morphologic deterioration and destruction in association with condensed granular structures positive for granzyme B. An accumulation of large numbers of ionized calcium binding adaptor molecule 1 (Iba1)$^+$ microglia and Ly6C$^+$ inflammatory macrophages was always detected within and around those destroyed cysts, and destroyed individual organisms were detectable within these infiltrated phagocytes. These studies uncovered a superior and aggressive effector capability of CD8$^+$ cytotoxic T cells to penetrate into *T. gondii* cysts and induce their elimination in collaboration with microglia and macrophages.

Materials and Methods

Mice

CBA/J, BALB/c, and BALB/c-background SCID mice were obtained from the Jackson Laboratories (Bar Harbor, ME). BALB/c-background athymic nude mice and Swiss-Webster mice were from Taconic (Germantown, NY). BALB/c-background perforin-knockout (*Prf1*$^{-/-}$) mice[11] were bred in our animal facility. Mouse care and experimental procedures were performed under pathogen-free conditions in accordance with established institutional guidance and approved protocols from the Institutional Animal Care and Use Committee. Female mice were used for all studies. There were three to seven mice in each experimental group.

Infection with *T. gondii*

The ME49 strain of *T. gondii* was maintained *in vivo* by infecting Swiss-Webster mice with 10 cysts intraperitoneally.[12,13] In the experiments described in the present study, cysts were obtained from brains of chronically infected Swiss-Webster mice and all experimental mice were infected with 10 or 20 cysts orally by gavage. SCID and nude

mice were treated with sulfadiazine in the drinking water (400 mg/L) beginning at 9 to 11 days after infection for the entire period of the experiments to inhibit the proliferation of tachyzoites and establish a chronic infection in their brains.[12,14] *Prf1*$^{-/-}$ mice received sulfadiazine beginning at 4 weeks after infection. CBA/J mice were divided into two groups after infection, and one group received sulfadiazine treatment beginning at 3 weeks after infection.

Purification and Transfer of CD8$^+$ T Cells

CD8$^+$ immune T cells were purified from the spleens of chronically infected BALB/c and *Prf1*$^{-/-}$ mice using magnetic bead—conjugated anti-mouse CD8 (53-6.7) monoclonal antibodies (Miltenyi Biotech, Auburn, CA), as described previously.[12,14] CD8$^+$ normal T cells were also purified from the spleens of uninfected BALB/c mice in the same manner. A total of 2.1 to 4.2 × 10^6 CD8$^+$ T cells were injected intravenously from a tail vein into sulfadiazine-treated SCID or nude mice at 3 weeks after infection.[12,15]

Real-Time RT-PCR

The brains of infected SCID mice were obtained after perfusion with 20 mL of phosphate-buffered saline (PBS; pH 7.2) at 7 days after a transfer of CD8$^+$ T cells, and RNA was isolated from a half of each brain, as described previously.[16,17] The total RNAs were pretreated with DNase I (Invitrogen, Carlsbad, CA), to remove genomic DNA contaminating the RNA preparations, and then applied for cDNA synthesis.[16,17] Real-time PCR for mouse β-actin, bradyzoite-specific BAG1, cyst wall glycoprotein (CST)1, and SAG2c, tachyzoite-specific SAG1, the T-cell marker CD3δ, IFN-γ, and the effector molecules (guanylate-binding protein 1, immunity-related GTPases M3, and inducible nitric oxide synthase 2) of IFN-γ—mediated protective immunity against tachyzoites was performed with the cDNA using the reagents from Applied Biosystems with the StepOnePlus real-time PCR system (Applied Biosystems, Branchburg, NJ).[18] The primers and probes for BAG1 and SAG1 were described previously.[19] The primers and probe for CST1 and SAG2c are as follows: 5′-CTTGTTACTGTTCCGCCT-TTCTG-3′ (forward), 5′-CGTCAAAGTCTTTACATCGTT-GCA-3′ (reverse), and 5′-TCCGGTCCAAGAAACC-3′ (probe) for CST1; and 5′-CGCACAGTCATTCAACCAAA-AAGTT-3′ (forward), 5′-TGGAGGTGACCGCTACAGT-3′ (reverse), and 5′-TTGTGTCGTTCAGATAAATG-3′ (probe) for SAG2c. Expression levels of mRNA for the molecules of interest were determined by relative ratios to mouse β-actin mRNA levels.

Immunohistochemistry

Sagittal sections (4 μm thick) of the brains were deparaffinized and rehydrated using xylene, ethanol, and then water. Heat-induced epitope retrieval (HIER) was performed in

citrate buffer (pH 6) within a microwave for 5 minutes. The slides were then treated with 3% H$_2$O$_2$ for 15 minutes and then blocked with 5% bovine serum albumin in Tris-buffered saline with 0.5% Tween 20 for 2 hours. All primary antibodies and secondary antibodies used for staining were diluted in 5% bovine serum albumin/Tris-buffered saline with 0.5% Tween 20, and the incubation with these antibodies was for 1 or 2 hours at room temperature or overnight at 4°C. Staining of slides for *T. gondii* and CD3 was performed as described previously.[20] Staining for bradyzoite-specific BAG1 and CD3 was performed in the same manner, with a modification of the use of mouse anti-BAG1 monoclonal antibody after blocking with F(ab)$_2$ fragments of goat anti-mouse IgG (Jackson ImmunoResearch Laboratories, West Grove, PA) overnight. The secondary antibody was horseradish peroxidase—conjugated goat anti-mouse IgG (Jackson ImmunoResearch Laboratories). Three-dimensional images were obtained by Zeiss Axio Imager M1 microscope (Zeiss, Oberkochen, Germany) using ZEN 2.0.0.0 pro software for regular light microscopy (Zeiss).

Staining for *T. gondii*, Iba1, and Ly6C was performed as follows. After the HIER and blocking, the slides were then incubated with goat anti-Iba1 antibody (Abcam, Cambridge, MA). The slides were washed in Tris-buffered saline with 0.5% Tween 20 and incubated with alkaline phosphatase—conjugated donkey anti-goat IgG antibody (Invitrogen). Color was developed using Vulcan Fast Red Chromogen (Biocare Medical, Pacheco, CA). The slides were then incubated with polyclonal rat anti—*T. gondii* serum,[20] and then after washing, they were incubated with horseradish peroxidase—conjugated donkey anti-rat IgG antibody (Jackson ImmunoResearch Laboratories). The slides were then washed, and color was developed with diaminobenzidine (Vector Laboratories, Burlingame, CA). The slides were then subjected to two more rounds of HIER to facilitate removal of the prebound antibodies used for the staining for Iba1 and *T. gondii*.[21] The slides were then reblocked and incubated with rat anti-Ly6C antibody (Abcam) and then the horseradish peroxidase—conjugated anti-rat IgG antibody. Thereafter, the slides were incubated with Vina Green Chromogen (Biocare Medical) for color development. Staining for CD3 (red), *T. gondii* (brown), and granzyme B (green) was performed in the same manner. Rabbit anti—granzyme B antibody was from Abcam.

Staining for *T. gondii*, CD3, glial fibrillary acidic protein, and neuronal nuclei (NeuN) was performed as follows. The staining of *T. gondii* and CD3 was performed as described earlier, with a slight modification by using alkaline phosphatase—conjugated goat anti-rabbit IgG antibody (Invitrogen). After the color development, the slides were subjected to two rounds of HIER to remove prebound antibodies, followed by reblocking, as described in the previous paragraph. The slides were then incubated with rabbit anti-NeuN antibody (Abcam), followed by incubation with the alkaline phosphatase—conjugated goat anti-rabbit IgG antibody. Color was developed using alkaline phosphatase substrate Vector Blue (Vector Laboratories). The slides were then incubated

with goat anti—glial fibrillary acidic protein antibody (Abcam), followed by incubation with the horseradish peroxidase—conjugated donkey anti-goat IgG antibody (Invitrogen) and color development with Vina Green Chromogen.

Immunofluorescence staining of a combination of *T. gondii* and granzyme B or CD3 was as follows. After HIER, the slides were washed in PBS with Tween 20, blocked in PBS with Tween 20 with 1% normal goat serum (Jackson ImmunoResearch) and 2.5% bovine serum albumin for 2 hours, and incubated simultaneously with a combination of rat anti—*T. gondii* and rabbit anti—granzyme B (Abcam) or rabbit anti-CD3 antibodies at 4°C overnight. The slides were washed in PBS with Tween 20 and incubated with the AlexaFluor-488—conjugated goat anti-rat and AlexaFluor-594—conjugated goat anti-rabbit antibodies (Jackson ImmunoResearch) at room temperature for 1 hour. After washing in PBS with Tween 20 and then in PBS, the slides were mounted with ProLong Diamond Antifade Mountant (Invitrogen). The aforementioned mountant was cured overnight at room temperature before fluorescent visualization. Confocal images were obtained by a Nikon A1R microscope (Nikon, Tokyo, Japan) using NIS Elements AR 4.50.00 software (Nikon).

Measurement of the Diameters of *T. gondii* Cysts

Four to five sections from the brain of each of four infected CBA/J mice were stained for *T. gondii* and CD3, and a digital image of each of the cysts detected on the sections was taken to measure the diameter of each cyst using NIS-Elements BR acquisition 3.2 (Nikon).

Statistical Analysis

Levels of significance between experimental groups were determined by *t*-test or *U*-test (IBM SPSS, Armonk, NY). When there were more than two groups in the comparison, the corrected *P* value was calculated by multiplying each *P* value by the number of comparisons performed among the groups. Levels of differences in frequencies of destroyed cysts in total cyst populations and those with and without association with granzyme B and Ly6C between groups were determined by the Fisher exact test (QuickCalcs 2x2; GraphPad Software, San Diego, CA). Differences that had *P* values or corrected *P* values (when these values were applied) < 0.05 were considered significant.

Results

Perforin-Mediated Activity of CD8$^+$ Immune T Cells Is Able to Remove Pre-Existing *T. gondii* Cysts from the Brain

CD8$^+$ immune T cells have a potent capability to reduce numbers of *T. gondii* cysts in the brains of mice through their perforin-mediated activity.[10] However, the perforin-

mediated activity of the CD8$^+$ T cells might be attributed to inhibiting proliferation of tachyzoites and, thereby, reduced numbers of cysts. Therefore, it was first addressed whether the reduction of cyst numbers induced by perforin-mediated activity of CD8$^+$ immune T cells is due to indirect effects from inhibiting cerebral tachyzoite growth. CD8$^+$ T cells purified from the spleens of infected wild-type (WT) BALB/c and Prf1$^{-/-}$ mice were intravenously injected into infected, sulfadiazine-treated SCID mice that lack T cells in the same manner as previously described.[12,15] Seven days after the cell transfer, markedly and significantly decreased amounts of mRNA for bradyzoite (cyst)-specific BAG1, CST1 (Figure 1A), and SAG2C (Supplemental Figure S1) were detected in the brains of the animals that had received the WT CD8$^+$ T cells but not of those that had received the

Prf1$^{-/-}$ CD8$^+$ T cells, when compared with the control mice that had received no T cells ($P < 0.001$). In addition, the mRNA levels for BAG1, CST1, and SAG2C in the Prf1$^{-/-}$ CD8$^+$ T-cell recipients were significantly greater than those of the WT T-cell recipients ($P < 0.05$) (Figure 1A and Supplemental Figure S1). To address whether Prf1$^{-/-}$ CD8$^+$ T cells efficiently migrated into the brains of the recipients, the amounts of mRNA for CD3 were measured in the brains of recipients. In the control mice that had not received any T cells, cerebral CD3 mRNA levels were low and close to the detectable limit, as expected (Figure 1B). In contrast, large amounts of CD3 mRNAs were detected in the brains of both WT and Prf1$^{-/-}$ T-cell recipients in a similar manner ($P < 0.001$ and $P < 0.01$, respectively) (Figure 1B). Thus, Prf1$^{-/-}$ CD8$^+$ T cells had
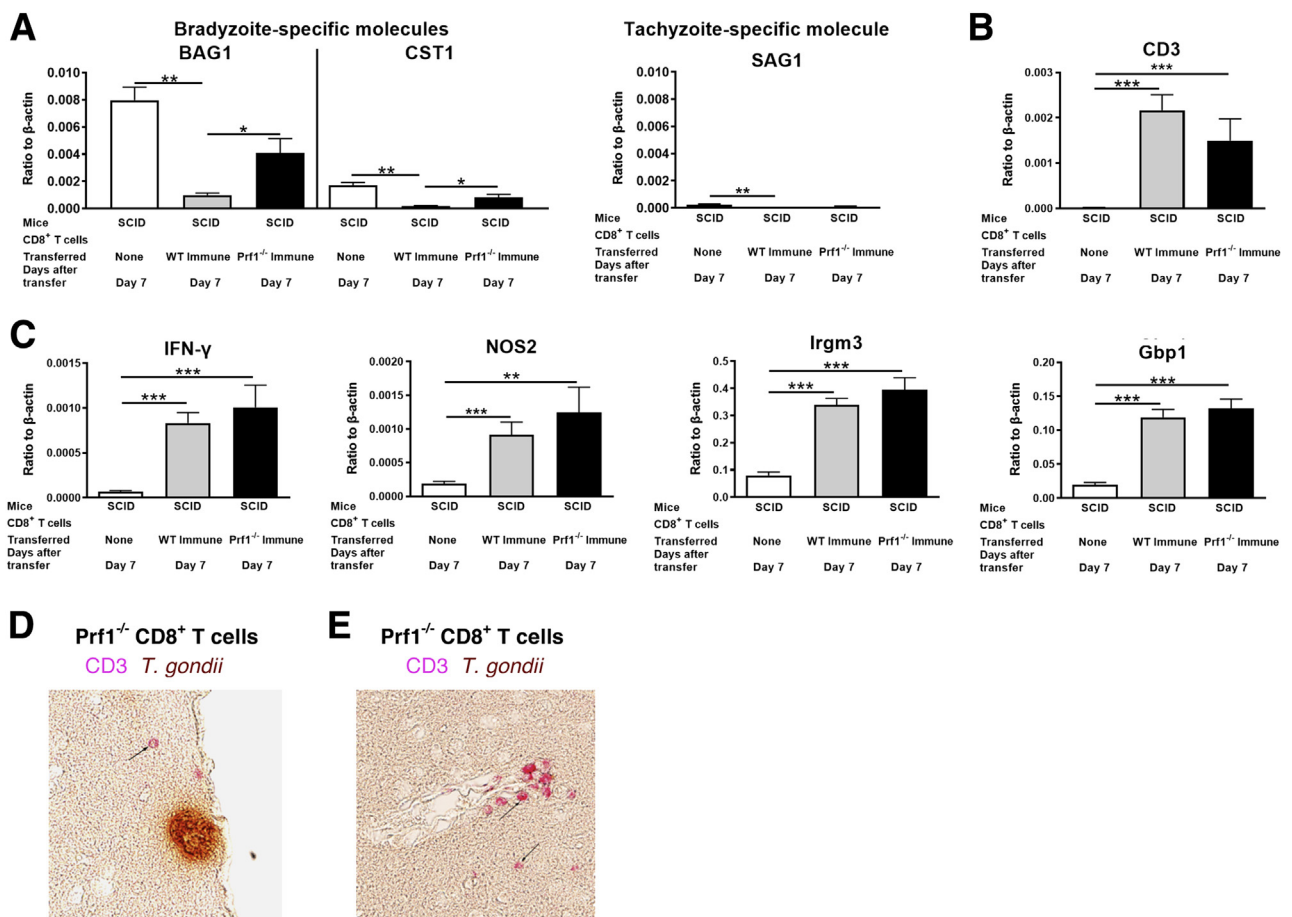

Figure 1 CD8$^+$ immune T cells eliminate pre-existing cysts of *Toxoplasma gondii* through perforin-dependent cytotoxic activity. Severe combined immunodeficiency (SCID) mice were infected orally with 10 cysts of the ME49 strain of *T. gondii* and treated with sulfadiazine beginning at 10 days after infection to establish a chronic infection by forming cysts in their brains. **A** and **B:** CD8$^+$ immune T cells (2.1×10^6 cells) purified from the spleens of chronically infected wild-type (WT) or Prf1$^{-/-}$ mice were injected intravenously from a tail vein, and 7 days later, amounts of mRNA for bradyzoite (cyst)-specific BAG1 and CST1 and tachyzoite-specific SAG1 (**A**) and CD3, a T-cell surface marker (**B**), were measured by real-time RT-PCR in the brains of the recipient animals. **C:** Amounts of mRNA for interferon (IFN)-γ and effector molecules [inducible nitric oxide synthase 2 (NOS2), immunity-related GTPases M3 (Irgm3), and guanylate-binding protein 1 (Gbp1)] of the IFN-γ—mediated protective immunity to prevent tachyzoite proliferation were also measured by real-time RT-PCR. *P* values were obtained using *t*-test, and corrected *P* values shown in the figure were calculated by multiplying the *P* values by the number of comparisons performed among three groups. **D** and **E:** Immunohistochemical detection of T cells in the parenchyma (**D**) and a perivascular area (**E**) of the brains of infected nude mice at 2 to 3 days after a systemic transfer of Prf1$^{-/-}$ CD8$^+$ immune T cells (4.2×10^6 cells). The T cells (positive for CD3) were stained in red. **Arrows** indicate the representatives of the T cells. Data are expressed as means ± SEM in each group (**A—C**). *$P < 0.05$, **$P < 0.01$, and ***$P < 0.001$. Original magnification, ×200 (**D** and **E**).

migrated into the brains of the recipients as efficiently as the WT CD8^{+} T cells. This point is further supported by the evidence that CD3^{+} T cells were detectable in the parenchyma (Figure 1D), including perivascular areas (Figure 1E), of the brains of infected nude mice at 2 to 3 days after a systemic transfer of $Prf1^{-/-}$ CD8^{+} immune T cells. These results confirmed that perforin is the major mediator of anticyst activity of CD8^{+} immune T cells to reduce bradyzoite burden in the brains of recipient mice. However, because cyst burden in the $Prf1^{-/-}$ T-cell recipients tended to be less than that of the control mice without any T-cell transfer (Figure 1A and Supplemental Figure S1), possible involvement of other mechanisms contributing to a lesser extent to the anticyst immune process, such as that mediated by chitinase-dependent activity of alternatively activated macrophages, cannot be excluded.[22]

To address whether the absence of perforin affected the activity of CD8^{+} immune T cells to prevent cerebral tachyzoite growth, amounts of mRNA were compared for tachyzoite-specific SAG1 in the brains of infected SCID mice that had received the WT or $Prf1^{-/-}$ CD8^{+} T cells.[10,20,23] In contrast to BAG1 mRNA levels, tachyzoite-specific SAG1 mRNA did not differ between the recipients of WT and $Prf1^{-/-}$ CD8^{+} T cells (Figure 1B). Furthermore, the amounts of SAG1 mRNA were 45 and 41 times less than those of BAG1 mRNA in both WT and $Prf1^{-/-}$ CD8^{+} T-cell recipients, respectively (Figure 1A). These results indicate that both WT and $Prf1^{-/-}$ CD8^{+} T cells effectively prevented tachyzoite growth in the brains of recipients to the same extent and that differences in cyst numbers were not attributable to differences in tachyzoite proliferation. Consistent with these findings, markedly increased mRNA levels for IFN-γ and the effector molecules (inducible nitric oxide synthase 2, immunity-related GTPases M3, and guanylate-binding protein 1) in the IFN-γ—mediated protective immunity to prevent tachyzoite growth[24–26] were detected in the brains of both of these two recipient groups in the same manner (Figure 1C). These results indicate that the reduction of T. gondii cyst burden by perforin-mediated activity of CD8^{+} T cells is due to direct removal of preexisting T. gondii cysts, rather than indirect effects from inhibiting tachyzoite proliferation.

T Cells Not Only Attach to the Surface of Host Cells Harboring *T. gondii* Cysts but Also Invade into the Cysts

To visualize the direct interactions of CD8^{+} T cells with *T. gondii* cysts, immunohistochemical studies were performed on the brains of infected mice. As the first step, to have better chances to detect the interactions of the T cells with cysts, a strain (CBA/J) of mice that forms large numbers of brain cysts after infection was used.[27,28] Sagittal sections (4 µm thick) of their brains were stained for T cells (CD3 for

the T-cell marker) in red and *T. gondii* in brown (Figure 2, A, B, D, E, G, and I). To confirm that the targets of the interaction with the T cells are the cyst stage of the parasite, staining was also performed for bradyzoite-specific BAG1 (brown) in combination with the staining for CD3 (red) (Figure 2, C, F, H, and J). A morphologic characteristic of *T. gondii* cysts is the glycan-rich cyst wall surrounding large numbers of bradyzoites (Supplemental Figure S2).[2–4] In the immunohistochemical staining, a number of cysts attached by T cells on their surface were observed (Figure 2, A—C). Because *T. gondii* cysts reside within host cells,[29] these results indicate that immune T cells of the chronically infected mice are able to recognize the host cells harboring the cysts and attach on the surface of these cells. The T cells that attached on the surface of the cyst-containing cells were not always in a regular round shape. Often, T cells displaying a spindle shape on the surface of cyst-containing cells were detected, as if they were trying to penetrate into the cysts (Figure 2B). Even when the T cells attached were round, multiple cysts whose cyst wall bent inward at the site of T-cell attachment were seen (Figure 2C), with a projection of the cyst wall outward nearby the site of the T-cell attachment (Figure 2C), suggesting that the attached T cells were making pressure to penetrate into the cyst. T cells were also observed spreading on the surface of cyst-containing cells (Figure 2A).

Consistent with the spindle shape of T cells attached on the surface of the cyst-containing cells, a number of T cells that had migrated halfway through the cyst wall were observed (Figure 2, D—F). Notably, a number of T cells were found located completely within the cysts (Figure 2, G and H). Because the thickness of the sections used for the staining was 4 µm, those T cells detected in Figure 2, G and H, were not on the surface of the cysts but within the cysts. These results indicate that T cells are capable of penetrating into the cysts of *T. gondii* in the brains of infected mice. A number of totally destroyed cysts were also detected (Figure 2, I and J). These destroyed cysts were always associated with an accumulation of inflammatory cells, including T cells (Figure 2, I and J). These results suggest that immune T cells have an aggressive invader capability to penetrate into the cysts by passing through the cyst wall for their destruction. The frequencies of the cysts attached by or invaded by T cells among a total number of cysts detected ranged from 11.4% to 22.6% among five mice, with the average of 16.2% (274 in a total of 1691) (Supplemental Figure S3), suggesting the presence of a large number of immune T cells that have anticyst activity in the brains of the infected mice.

T Cells Attack *T. gondii* Cysts Regardless of the Size of the Cysts

To determine whether anticyst T cells attack the cysts of a particular size, the diameters of all of 249 cysts that had evidence of T-cell attachment or invasion (excluding those deteriorated or destroyed) in four to five sections from the
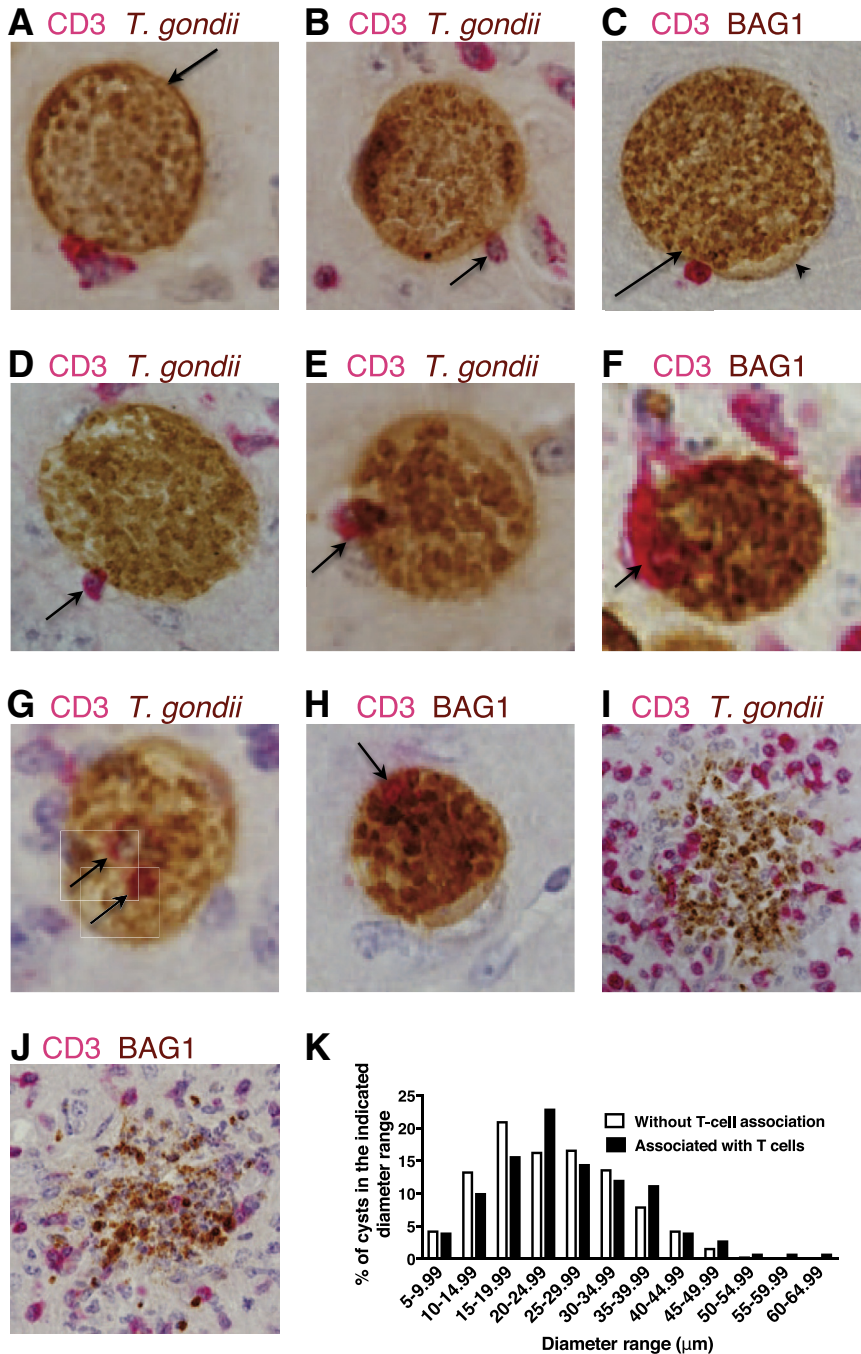
Figure 2 Invasion of T cells into *Toxoplasma gondii* cysts in the brains of infected mice. **A–J:** CBA/J mice were infected orally with 10 cysts of the ME49 strain of *T. gondii*; and 2 months later, their brains were applied for immunohistologic staining for *T. gondii* (**A**, **B**, **D**, **E**, **G**, and **I**) or bradyzoite-specific BAG1 (**C**, **F**, **H**, and **J**) in brown in combination with the staining for CD3, the T-cell marker, in red. The entire fields of four or five sagittal sections from each of the brains of four mice were analyzed. **A–C:** T cells that attached on the surface of cyst-containing cells. **A:** An **arrow** indicates the cyst wall. **B:** The **arrow** indicates the T cells in a spindle shape. **C:** The **arrow** indicates the bent of cyst wall inward at the site of T-cell attachment, and the **arrowhead** indicates a projection of the cyst wall outward nearby the site of the T-cell attachment. **D–F:** T cells located halfway through the cyst wall (**arrows**). **G** and **H:** T cells completely penetrated into the cysts were detected (**arrows**). **I** and **J:** Totally destroyed cysts associated with an accumulation of inflammatory cells, including T cells. **K:** Comparison of the diameters of cysts with and without T-cell association. Original magnification: ×400 (**A–H**); ×200 (**I** and **J**).

brain of each of four mice was measured. The diameters were also measured for 300 cysts randomly selected from the cysts without T-cell association in the same sections, in which the diameters of the T-cell–associated cysts were measured. The attachment and penetration of T cells were observed on the cysts of a wide range of different sizes. The distributions of the sizes of cysts with an association with T cells were similar to those without the T-cell association (Figure 2K). These results indicate that T cells are able to detect cyst-containing cells regardless of the size of the cysts to induce their elimination.

CD8$^+$ Subset of Immune T Cells Penetrates into *T. gondii* Cysts

To determine whether the CD8$^+$ subset of the T cells has the capability to invade into *T. gondii* cysts, CD8$^+$ immune T cells purified from the spleens of infected WT BALB/c mice were intravenously injected from a tail vein into infected nude mice. As a control, infected nude mice received CD8$^+$ normal T cells purified from uninfected WT mice. At 2 and 3 days after the cell transfer, many cysts attached by CD8$^+$ T cells were detected in the brains of

mice that had received the immune T cells (Figure 3, A and B). A portion of those CD8$^+$ T cells were in a spindle shape (Figure 3A), which is consistent with the T cells observed in the brains of infected CBA/J mice shown in Figure 2B. In addition, leakage of *T. gondii* materials was detected at the site that the T cells tightly attached (Figure 3G). In Figure 3H, leakage of the parasite materials is more clearly visible, along with a bend of the cyst wall inward at the site of the T-cell attachment.

CD8$^+$ immune T cells that had migrated halfway through the cyst wall were also detected (Figure 3, C and D). Confocal images of a T cell that had migrated halfway into a cyst are also shown in Figure 3, I−K. An overlap of both green (*T. gondii*) and red (CD3) is clearly visible in the merged image (Figure 3K). Cases of multiple CD8$^+$ T cells simultaneously located halfway through the cyst wall of a single cyst were also detected (Figure 3, E and F), and some of these T cells were located totally within the cysts
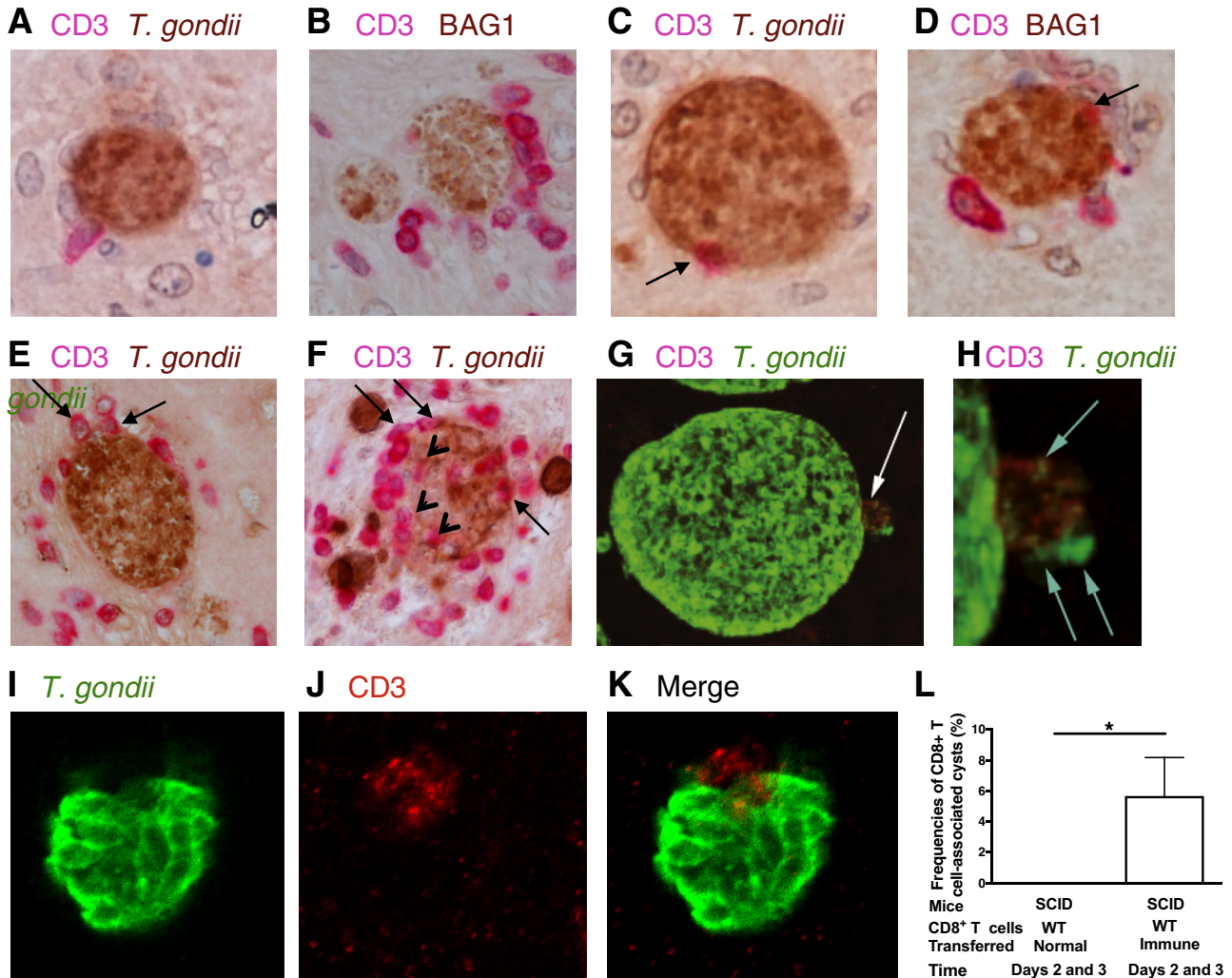

Figure 3 CD8$^+$ immune T cells attach to and invade into *Toxoplasma gondii* cysts in the brains of infected mice. Athymic nude mice were infected orally with 20 cysts of the ME49 strain of *T. gondii* and treated with sulfadiazine beginning at 11 days after infection to establish a chronic infection by forming cysts in their brains. **A−F:** CD8$^+$ T cells (3.5 × 10^6 cells) purified from the spleens of infected BALB/c mice were injected intravenously from a tail vein; and 2 to 3 days later, their brains were applied for immunohistochemical staining for *T. gondii* (brown; **A, C, E,** and **F**) or bradyzoite-specific BAG1 (brown; **B** and **D**) and CD3 (red), the T-cell marker. **A** and **B:** T cells attached on the surface of cyst-containing cells. **C−F:** T cells that had migrated halfway through the cyst wall (**arrows**). **F:** T cells that completely penetrated into the cysts were detected (**arrowheads**). **G−K:** Confocal microscopy with staining for *T. gondii* (green) and CD3 (red) was also performed on their brains. **G:** The bent of the cyst wall inward at the site of CD8$^+$ T-cell attachment (**arrow**). **H:** Leakage of *T. gondii* materials at the site of CD8$^+$ T-cell attachment (**arrows**), shown at higher magnification in **H. H:** Leakage of *T. gondii* materials at the site of CD8$^+$ T-cell attachment (**arrows**). **I−K:** Confocal images of the T cell that was halfway in the invasion into a cyst. Another group of infected and sulfadiazine-treated nude mice received CD8$^+$ normal T cells from uninfected BALB/c mice, and the immunohistochemical studies were performed on their brains in the same manner. **L:** The frequencies of *T. gondii* cysts associated with the T cells were calculated for each of these two groups of mice that had received the normal or immune CD8$^+$ T cells. Data are expressed as means ± SEM in each group (**L**). *$P < 0.05$ (*U*-test). Original magnification: ×400 (**A−F**); ×1000 (**G−K**). SCID, severe combined immunodeficiency; WT, wild type.

(Figure 3F). There were usually no other cells, or a few if any, detected on the surface of those cysts attached or invaded by CD8$^+$ T cells (Figure 3, B, C, and E), suggesting that CD8$^+$ immune T cells are the first immune cell population that attacks the cysts. The frequency of CD8$^+$ T-cell–associated cysts among the overall population of cysts detected ($n = 177$) was 5.7% in the brains of animals ($n = 7$) that had received the immune T cells (Figure 3L). In contrast, none of the cysts ($n = 161$) were associated with T cells in the brains of the control mice ($n = 6$) that had received CD8$^+$ normal T cells ($P < 0.05$) (Figure 3L).

To further confirm the invasion of CD8$^+$ immune T cells into *T. gondii* cysts, three-dimensional images of the cysts invaded by the T cells were obtained by obtaining Z-stack images using light microscopy. In the cysts shown in Figure 4, the presence of the T cells is clearly visible in the images taken at both the top and the bottom of the histologic sections. Furthermore, the Z-stack three-dimensional images (Figure 4) generated at the cut line indicated in green on the top images (Figure 4) show the presence of the T cells within these cysts all of the way through the thickness of the sections. Supplemental Figure S4 provides additional images of a cyst invaded by T cells. In this cyst, the cyst wall is visible all around the cyst, and the T cell is located within this cyst. These results clearly indicate that these T cells were not located on the surface of the cysts but were present within the cysts.

Invasion of CD8$^+$ Immune T Cells Induces Deterioration of *T. gondii* Cysts in Association with Granular Materials Containing Granzyme B

Consistent with the observation on the cysts in infected CBA/J mice, the cysts invaded by CD8$^+$ immune T cells in the brains of nude mice that had received the T cells were often not maintaining a typical circular shape and were morphologically deteriorated or destroyed (Figure 5, A and B). The frequencies of destroyed cysts among total cysts detected in 15 sections of the brains of six mice were 2.3% (26/1146) (Figure 5C), which is significantly higher than that in the brains of nude mice that had received normal CD8$^+$ T cells (0.35%, 4/1135 in 18 sections in 8 mice; $P < 0.001$) (Figure 5C). This observation is consistent with the evidence that an attachment of CD8$^+$ T cells on cysts was detectable only in the brains of mice that had received the immune T cells, as shown in Figure 3L. These data strongly suggest that most of the destruction of cysts is caused by attack from CD8$^+$ immune T cells.
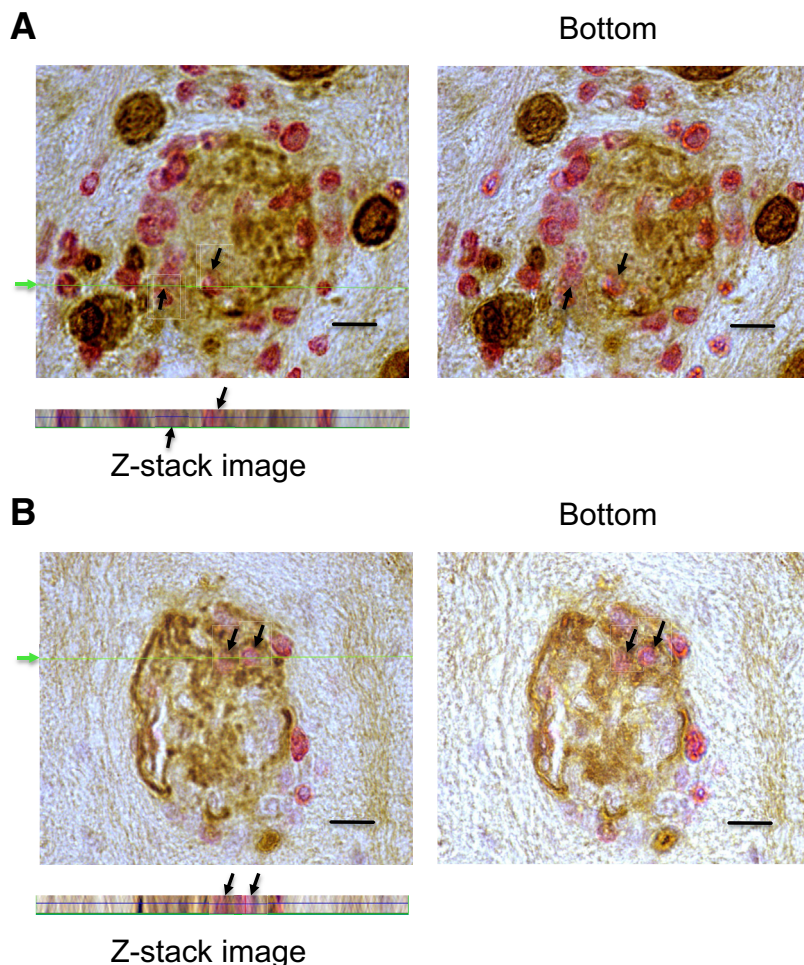
Figure 4 The three-dimensional (3-D) images of *Toxoplasma gondii* cysts containing CD8$^+$ T cells that had fully invaded into the cysts. Nude mice were infected orally with 20 cysts of the ME49 strain of *T. gondii* and treated with sulfadiazine beginning at 11 days after infection to establish a chronic infection by forming cysts in their brains. CD8$^+$ T cells (3.5×10^6 cells) purified from the spleens of infected BALB/c mice were injected intravenously from a tail vein; and 2 to 3 days later, their brains were applied for immunohistochemical staining for *T. gondii* (brown) and CD3 (red) and Z-stack images were obtained using light microscopy. **Top rows:** The images taken at the top and bottom of the histologic sections. The presence of the T cells (**arrows**) can be seen in both images at the top and bottom of the sections. **Bottom panels:** 3-D images generated from the Z-stack images of the cysts at the cut line, indicated by a **green arrow** and **line**. These Z-stack images demonstrate the presence of the T cells (**arrows**) all of the way through the sections. Scale bars = 10 μm (**A** and **B**). Original magnification, ×1500 (**A** and **B**, **bottom rows**).
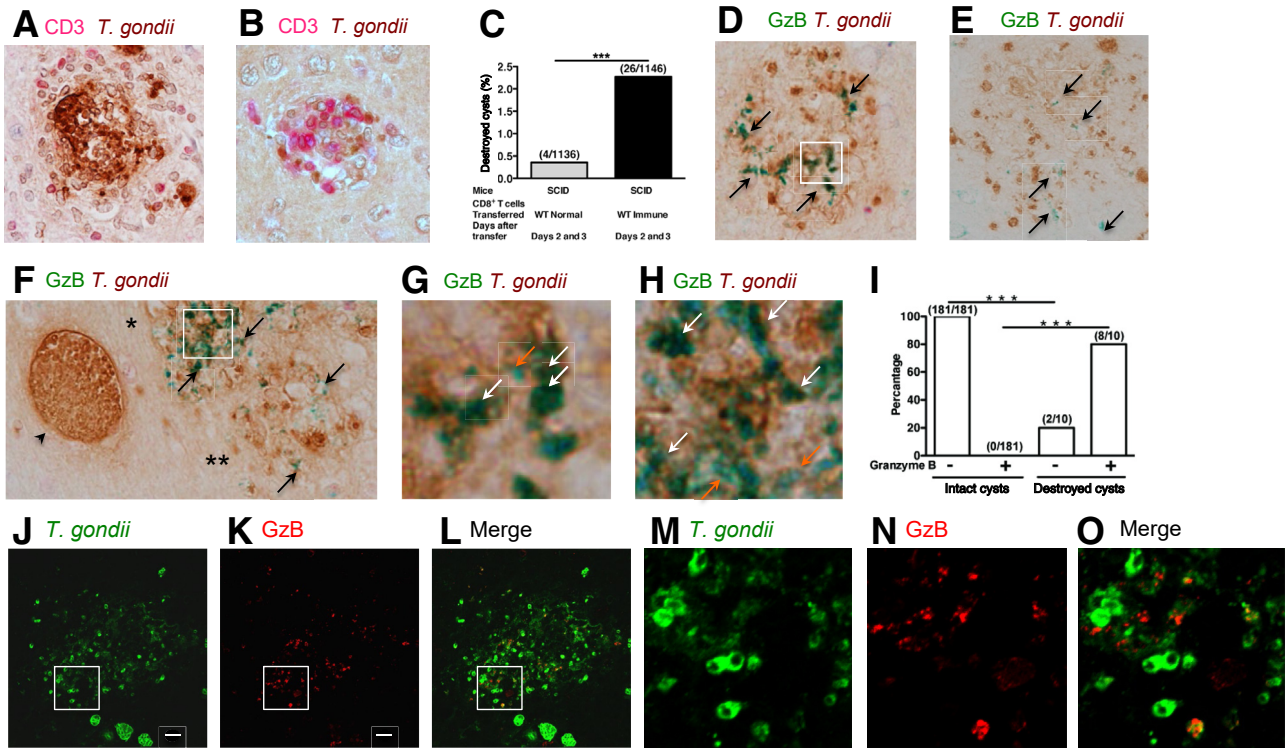
Figure 5 Penetration of CD8$^+$ immune T cells into *Toxoplasma gondii* cysts induces morphologic deterioration of the cysts, and their destruction is associated with granular materials with a high density of granzyme B (GzB). Nude mice were infected orally with 20 cysts of the ME49 strain of *T. gondii* and treated with sulfadiazine beginning at 11 days after infection to establish a chronic infection by forming cysts in their brains. CD8$^+$ immune T cells (3.5 × 10^6 cells), purified from the spleens of infected BALB/c mice, were injected intravenously from a tail vein; and 2 to 3 days later, their brains were applied for immunohistochemical staining for *T. gondii*. **A** and **B:** CD8$^+$ T-cell—invaded cysts displaying morphologic deterioration and destruction. CD3 is in red, and *T. gondii* is in brown. **C:** The frequencies of destroyed cysts in the brains of nude mice at 2 to 3 days after receiving either CD8$^+$ normal or immune T cells. **D—F:** The presence of granular staining of granzyme B (green; **arrows**) in the areas of destroyed cysts (brown). **Boxed areas** in **D** and **F** are seen at higher magnification in **G** and **H**, respectively. **F:** An **arrowhead** indicates an intact cyst adjacent to the destroyed cysts. **Single** and **double asterisks** indicate two independent cysts destroyed with the presence of different amounts of granular structures positive for granzyme B and different intensities of granzyme staining. **G** and **H:** Many of the granular structures positive for granzyme B within destroyed cysts were in dark green color (**white arrows**), resulting from a mixture of green (the color used for staining granzyme B) and brown (the color used for staining *T. gondii*), when compared with staining showing only green (**orange arrows**). **I:** The frequencies of granular structures positive for granzyme B within destroyed cysts and morphologically intact cysts. **J—O:** Immunofluorescence staining of destroyed cysts for granzyme B (red) and *T. gondii* (green). The granular structures containing both granzyme B and *T. gondii* are seen in yellow because of the presence of both green and red. **Boxed areas** in **J—L** are seen at higher magnification in **M—O**. ***$P < 0.001$. Scale bars = 10 μm (**J** and **K**). Original magnification: ×400 (**A**, **B**, and **D—H**); ×1000 (**J—O**). SCID, severe combined immunodeficiency; WT, wild type.

To further address that the cyst destruction is through the cytotoxic activity of CD8$^+$ immune T cells, it was examined whether granzyme B is detectable within the destroyed cysts in the brains of mice with a CD8$^+$ immune T-cell transfer. Granzyme B is one of the cytotoxic proteins that CD8$^+$ cytotoxic T cells secrete into the targets during their attack on the targets. Granular structures intensely positive for granzyme B (Figure 5, D—F) were detected within most destroyed cysts (8/10) (Figure 5I). The absence of granzyme B in 2 of the 10 destroyed cysts does not mean that their destruction is not mediated by cytotoxic T-cell activity because the granzyme B—positive structures could be located within those destroyed cysts at the level either above or/and below the position that these sections were made for immunohistochemical staining.

The amounts of granzyme B—positive structures and the intensity of granzyme B staining varied among the destroyed cysts (Figure 5D versus Figure 5E), and the destroyed cyst indicated with one asterisk versus the destroyed cyst indicated with two asterisks (Figure 5F). There was a tendency that greater amounts and more intense staining of granzyme B were detectable within the destroyed cysts that had clear morphologies of individual bradyzoites and stronger color (brown) for their staining (Figure 5D versus Figure 5E) and the destroyed cyst indicated with one asterisk versus the destroyed cyst indicated with two asterisks (Figure 5F), suggesting that the volumes of the granular structures and the amounts of granzyme B in the granular structures decrease when destruction of bradyzoites within the cysts progresses. More importantly, this granzyme B staining was not detected in any of intact cysts, such as the one (Figure 5F) adjacent to the destroyed cysts (0/181; $P < 0.001$) (Figure 5I). These results along with the requirement of perforin for the activity of CD8$^+$ T cells to eliminate *T. gondii* cysts shown in Figure 1 strongly suggest that CD8$^+$ immune T cells use their cytotoxic activity to

destroy *T. gondii* cysts in the brains of infected mice. Because the amounts of the granular materials containing granzyme B within the destroyed cysts were large, CD8$^+$ cytotoxic T cells appear to secrete large amounts of granzyme B into cysts during their invasion and destruction of the cysts.

### Granzyme B Binds Bradyzoites within Destroyed Cysts

Because granzyme B is a serine protease, it is possible that this enzyme secreted by CD8$^+$ cytotoxic T cells during cyst destruction binds to bradyzoites and participates in the killing and destruction of the parasite. Many of the granular structures positive for granzyme B within destroyed cysts were in dark green (Figure 5, G and H), displaying enlarged images of the area indicated (Figure 5, D and F), respectively, suggesting a coexistence of green (the color used for staining granzyme B) and brown (the color used for staining *T. gondii*), when compared with staining showing only green (Figure 5, G and H). Immunofluorescence staining further confirmed that many of these granular materials positive for granzyme B are also positive for *T. gondii* antigens (Figure 5, J–O). Figure 5, J–L, displays an entire area of one destroyed cyst stained for *T. gondii* in green and granzyme B in red. Figure 5, M–O, displays enlarged images of the area indicated in Figure 5, J–L, in which much of granzyme B staining colocalized with the parasite. There was a tendency that fainter staining for the granzyme B is colocalized with fainter staining for *T. gondii*, suggesting that these granzyme B–bound bradyzoites had been in the process of destruction and degradation.

Prf1$^{-/-}$ CD8$^+$ Immune T Cells Attach to Cysts but Do Not Invade into or Destroy Cysts

Because perforin is crucial for anticyst activity of CD8$^+$ immune T cells (Figure 1), immunohistologic analyses were performed to examine at what step in the cyst removal process CD8$^+$ T cells are stalling in the absence of perforin. Infected nude mice received CD8$^+$ immune T cells from infected WT and *Prf1*$^{-/-}$ mice, and 2 to 3 days later, immunohistochemical staining was performed for *T. gondii*, CD3, and granzyme B. Although *T. gondii* cysts attached by T cells (Figure 6A) were frequently (6.5%, 6 of 93 total cysts detected) observed in the brains of the recipients of *Prf1*$^{-/-}$ CD8$^+$ T cells, no cysts invaded by the T cells or destroyed cysts associated with the granular structures positive for granzyme B were detected. In the brains of the recipients of WT CD8$^+$ T cells, destroyed cysts were detected; and the granular structures positive for granzyme B were detectable (Figure 6B), as observed in the studies shown in Figure 4. On the other hand, in the recipients of the *Prf1*$^{-/-}$ T cells, a cyst surrounded by the materials positive for granzyme B located outside of the cyst wall was observed (Figure 6A). Therefore, *Prf1*$^{-/-}$ CD8$^+$ immune T cells are able to recognize and attach to the surface of cyst-

A   *Prf1*$^{-/-}$ CD8$^+$ T- cell recipients

CD3 *T. gondii* GzB   CD3 *T. gondii* GzB
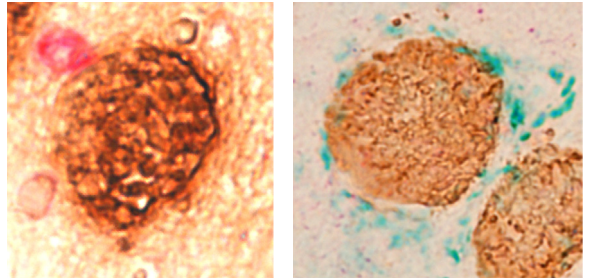
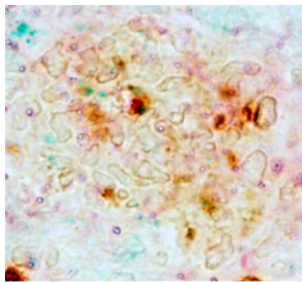## B WT CD8$^+$ T- cell recipient

CD3 *T. gondii* GzB

Figure 6   *Prf1*$^{-/-}$ CD8$^+$ T cells attach to cyst-containing cells but do not invade into or destroy cysts. Nude mice were infected with 20 cysts of the ME49 strain of *Toxoplasma gondii* and treated with sulfadiazine beginning at 9 days after infection to establish a chronic infection by forming cysts in their brains. CD8$^+$ T cells (4.2 × 10^6 cells) purified from the spleens of infected wild-type (WT) and *Prf1*$^{-/-}$ mice were injected intravenously from a tail vein. At 2 to 3 days after the T-cell transfer, their brains were applied for immunohistochemical staining for *T. gondii* (brown), CD3 (red), and granzyme B (GzB; green). **A: Left panel:** Attachment of *Prf1*$^{-/-}$ CD8$^+$ T cells on a cyst-containing cell. **Right panel:** A cyst surrounded by the materials positive for granzyme B located outside of the cyst wall in the brain of the *Prf1*$^{-/-}$ CD8$^+$ T-cell recipient. **B:** A destroyed cyst associated with the granular structures positive for granzyme B in the brain of the WT CD8$^+$ T-cell recipient. Original magnification, ×400 (**A** and **B**).

containing cells and most likely release granzymes from their granules. However, because of the absence of perforin that forms pores on the surface membrane of targets, the released granzymes stay adjacent to (outside of) cyst-containing cells.

Destruction of Cysts Is Associated with an Accumulation of Iba1$^+$ Microglia and Ly6C$^+$ Inflammatory Macrophages

Toxoplasma gondii forms cysts within neurons and astrocytes in the brains of infected hosts.[29,30] Destroyed cysts associated with the diffuse presence of NeuN, a marker of neurons (Figure 7A), and glial fibrillary acidic protein, a marker of astrocytes (Figure 7B), were detected in the brains of infected nude mice that had received WT CD8$^+$ immune
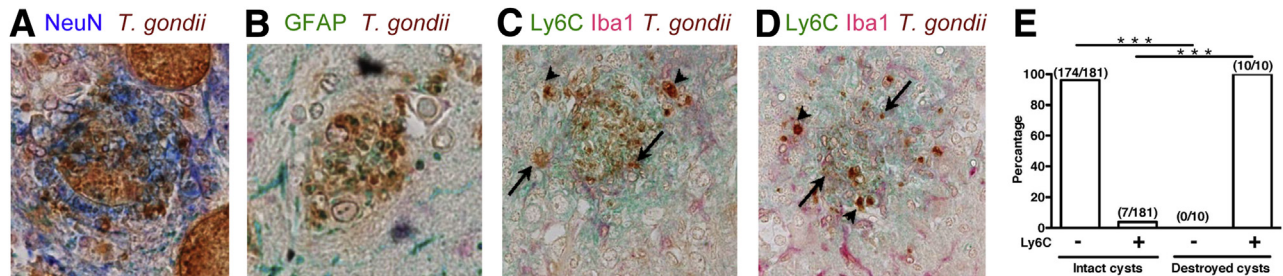
Figure 7   Both cysts formed within neurons and astrocytes were destroyed by CD8^{+} immune T cells, and the destruction of the cysts was associated with accumulation of Iba1^{+} microglia and Ly6C^{+} inflammatory macrophages. Nude mice were infected orally with 20 cysts of the ME49 strain of *Toxoplasma gondii* and treated with sulfadiazine beginning at 11 days after infection to establish a chronic infection by forming cysts in their brains. CD8^{+} T cells (3.5×10^6 cells) purified from the spleens of infected BALB/c mice were injected intravenously from a tail vein; and 2 to 3 days later, their brains were applied for immunohistochemical staining for *T. gondii*. **A** and **B:** Destroyed cysts (brown) associated with the presence of diffuse NeuN (blue; **A**) and glial fibrillary acidic protein (GFAP; green; **B**). **C** and **D:** Accumulation of Iba1^{+} microglia (red) and Ly6C^{+} blood-derived macrophages (green) is associated with demolished cysts (brown). **Arrowheads** indicate *T. gondii* parasites that maintain a clear morphology. **Arrows** indicate the representatives of the parasites that had already been destroyed and lost a clear morphology of the parasite. **E:** The differences in the frequencies of an accumulation of Ly6C^{+} macrophages to morphologically destroyed and intact cysts. ***$P < 0.001$. Original magnification, ×400 (**A–D**).

T cells, suggesting that the CD8^{+} immune T cells are able to attack both neurons and astrocytes that are harboring cysts. Most inflammatory cells that accumulated to destroyed cysts in their brains were identified as Iba1^{+} microglia and Ly6C^{+} blood-derived macrophages (Figure 7, C and D). Most, if not all, of *T. gondii* organisms were detected within these microglia and macrophages in the areas of cyst destruction. Portions of the *T. gondii*−positive materials located within the microglia and macrophages did not display a clear morphology of the parasite (Figure 7, C and D), in comparison with the parasite that maintained a clear morphology, suggesting that they had been destroyed within these phagocytes. Therefore, the microglia and macrophages are most likely the scavenger cells that eliminate the bradyzoites once CD8^{+} immune T cells invaded into the cysts and displayed cytotoxic anticyst effector functions. This possibility is supported by the fact that the accumulation of Ly6C^{+} macrophages was noticed in all (10/10) of the destroyed cysts detected (Figure 7E), whereas most (96.1%, 174/181) of morphologically intact cysts were observed without any association with these phagocytes (Figure 7E). The undestroyed cysts associated with Ly6C^{+} macrophages (3.9%, 7/181) could have been under an attack by the T cells, although they still maintain the intact morphology of cysts. This possibility is supported by a fact that a total (6.2%) of the frequency of destroyed cysts (2.3%) and that of the undestroyed cysts associated with Ly6C^{+} macrophages (3.9%) becomes close to the frequency of cysts attached or invaded by CD8^{+} immune T cells, which was 5.7% (Figure 3G).

Discussion

The present study identified that perforin-mediated activity of CD8^{+} immune T cells is capable of efficiently eliminating the pre-existing cyst form of *T. gondii* by using a previously unrecognized aggressive invasion capability in the brains of infected mice. Adoptive transfer of CD8^{+} immune T cells from WT and *Prf1*^{−/−} mice into infected T-cell−deficient mice revealed that only the former were able to reduce the cyst burden despite both of these T cells efficiently migrating into the brains of recipients and activating IFN-γ−mediated protective immunity to prevent cerebral proliferation of tachyzoites. More importantly, it was discovered that WT CD8^{+} immune T cells penetrate into *T. gondii* cysts during the cyst elimination immune process. The invasion of the T cells was associated with morphologic deterioration and destruction of the cysts. Notably, granular structures intensely positive for granzyme B were detected within most of the destroyed cysts. Both perforin and granzyme B are among the molecules secreted from cytotoxic T cells against targets during their attack of the targets. To our knowledge, the invasive effector capability of CD8^{+} cytotoxic T cells to directly penetrate into a target has not been reported before. *Toxoplasma gondii* cysts can grow into the size of >50 μm in their diameter. The present study uncovered a novel effector execution system of the protective immunity to eliminate those large targets, which is operated by an invasion of CD8^{+} cytotoxic T cells into a target of large mass.

Toxoplasma gondii cysts reside within infected host cells. Therefore, CD8^{+} cytotoxic T cells first need to recognize *T. gondii* antigen(s) presented by the major histocompatibility complex class I molecules on the surface of the cyst-harboring cells. Our recent studies identified that the N-terminus region of dense granule protein 6 of the *T. gondii*, presented by the H-2L[d] molecule, is a key target for CD8^{+} T cells to display their cytotoxic activity[31]; and that N-terminus region of dense granule protein 6−primed CD8^{+} T cells are able to reduce numbers of cysts in the brain when transferred to infected SCID mice that had already established large numbers of cysts.[31] Therefore, it is most likely that the recognition of the N-terminus region of dense granule protein 6 presented by the H-2L[d] molecule on the surface of cyst-containing cells by CD8^{+} cytotoxic T cells plays a critical role for their attachment to initiate their invasion into the cysts.

The present study illustrated that CD8^{+} immune T cells penetrate into the cysts by passing through the cyst wall. The cyst wall derives from the parasitophorous vacuole,[32] which is formed from host cell plasma membrane during the penetration of the parasite into the host cells.[33] Therefore, it is possible that the cyst wall contains the major histocompatibility complex class I molecules originally expressed on the surface of the plasma membrane of host cells. These major histocompatibility complex class I molecules on the cyst wall might be able to bind *T. gondii* epitopes produced by the processing of *T. gondii* antigens by the proteasome and cytosolic proteases in the cytoplasm of the cyst-containing cells, and CD8^{+} cytotoxic T cells recognize these epitopes presented on the surface of the cyst wall to penetrate into the cysts. Another possibility on how the CD8^{+} T cells trigger their penetration through the cyst wall would be that perforin, granzyme B, and/or other cytotoxic proteins released from the T cells into cyst-containing cells bind to the surface of the cyst wall and that the presence of large amounts of perforin and the other secreted cytotoxic proteins on the cyst wall surface triggers the invasion of the CD8^{+} T cells into these targets.

The present study revealed leakage of *T. gondii* materials from the site of CD8^{+} T-cell attachment. The leak of *T. gondii* antigens indicates that T cells are not simply attaching on the surface of the cyst wall but actively causing damage to the cyst wall. This evidence strongly suggests that CD8^{+} T cells use their perforin-mediated cytotoxic activity not only against cyst-containing cells but also against *T. gondii* cysts and that the pore-forming activity of perforin causes damage of the cyst wall. This damage of the cyst wall most likely aids penetration of the CD8^{+} T cells into the cysts. The observation of bending of the cyst wall inward is most likely due to the pressure extended by the CD8^{+} T cells in penetration into the cysts.

The destroyed cysts in the brains of mice with CD8^{+} immune T-cell transfer were identified in association with granzyme B—positive granular structures and filled with large numbers of Iba1^{+} microglia and Ly6C^{+} inflammatory macrophages. Granzyme B is a serine protease involved in the killing of target cells by cytotoxic T cells, as mentioned earlier. This molecule has also been shown to be involved in an induction of inflammation.[34] Therefore, granzyme B could contribute, at least in part, to inducing an accumulation of these microglia and macrophages after CD8^{+} cytotoxic T cells invade into the cysts. It is also possible that the serine-protease activity of granzyme B contributes to killing of bradyzoites and facilitates phagocytic removal of the killed bradyzoites by the accumulated phagocytes. In support of this concept, we have recently demonstrated that treatment of infected nude mice, which had received CD8^{+} immune T cells, with chloroquine (an inhibitor of endolysosomal acidification) at least partially inhibited CD8^{+} T-cell—mediated cyst removal.[35] It is probable that microglia and macrophages phagocytose bradyzoites and eliminate them by phagolysosome acidification, once CD8^{+} T cells have penetrated into the cysts and displayed their cytotoxic activities. Thus, the effector capability of invasive CD8^{+} cytotoxic T cells can be markedly amplified by large numbers of the accumulating phagocytes to eradicate the targets.

The frequencies of cysts attached by CD8^{+} immune T cells and destroyed cysts among the total cyst population were 5.7% and 2.3%, respectively, at the time points only 2 and 3 days after a systemic transfer of these T cells. A recent study using murine brain tumor models demonstrated that antigen-experienced, tumor-specific CD8^{+} effector T cells proliferate within brain parenchyma and further differentiate locally exhibiting enhanced IFN-γ and granzyme B expression.[36] Local expansion of cytotoxic effector CD8^{+} T cells was also reported in the liver in chronic hepatic viral infection.[37] Therefore, it is possible that *T. gondii* cyst-specific CD8^{+} cytotoxic T cells proliferate and differentiate locally in the brain and accelerate the cyst elimination during longer periods of time. This possibility is supported by the evidence that there is 95% reduction in cyst numbers at 1 month after a transfer of immune T cells in our previous study.[10] Therefore, the invasive effector function of CD8^{+} cytotoxic T cells, which is accompanied by an accumulation of large numbers of phagocytes, appears to be a novel and efficient mechanism of the immune system.

The Z-stack three-dimensional images clearly visualized the presence of CD8^{+} immune T cells within *T. gondii* cysts in the present study. Previous studies by others using a two-photon microscope were unable to depict the live images of CD8^{+} T-cell invasion into the cysts.[38,39] The strain of mice (C57BL/6) used in these studies could be one of the reasons for the unsuccessful detection of live images on the active interactions and invasion of anticyst CD8^{+} T cells with the cysts. In the present study, the CD8^{+} T-cell transfer studies were performed in BALB/c-background mice, which are genetically resistant to chronic *T. gondii* infection.[27,28] H-2L[d] is the critical antigen-presenting molecule for CD8^{+} T cells to recognize cyst-containing cells and eliminate the cysts.[31] C57BL/6 mice do not have the H-2L molecule. Therefore, CD8^{+} T cells attack *T. gondii* cysts possibly much less frequently in C57BL/6 mice than BALB/c mice. In addition, among the strains susceptible for chronic infection with *T. gondii*, C57BL/6 mice form fewer cysts in their brains than CBA/J mice, which is another strain used in the present study and allowed examination of a total of >1600 cysts (Figure 2). With the use of C57BL/6 mice, it would not be possible to examine this large number of cysts in live images with two-photon microscopy. In contrast, with the use of the light microscopy approach used in the present study, large amounts of time were spent in preparing sections of the brains and performing immunohistochemical analyses, which allowed reliable detection of the invasive effector activity of CD8^{+} T cells against the cysts.

The cytotoxic activity of CD8^{+} T cells is known to play important roles in the protective immunity against not only various intracellular microorganisms but also cancers. The

presence of CD8$^+$ T cells infiltrated into different types of solid cancers has been observed, and the presence of tumor-infiltrating T cells is an indicator of positive prognosis.[40] It is possible that these tumor-infiltrating CD8$^+$ T cells are, at least in part, aggressive penetrator CD8$^+$ T cells that invade the tumor using their perforin-mediated activity. The invasion of the T cells into tumors could induce an infiltration of large numbers of proinflammatory effector macrophages capable of attacking the cancer cells, as observed in the present study against *T. gondii* cysts. Therefore, effective activation of the aggressive and penetrating capability of CD8$^+$ cytotoxic T cells, revealed in the present study on *T. gondii* cysts, may be an important and powerful immunologic intervention that can also attack the other large targets, such as solid cancers, to induce their elimination.

Acknowledgment

Supplemental Data

Supplemental material for this article can be found at *http://doi.org/10.1016/j.ajpath.2019.04.018*.

References

1. Montoya JG, Liesenfeld O: Toxoplasmosis. Lancet 2004, 363: 1965−1976
2. Dubey JP, Lindsay DS, Speer CA: Structures of Toxoplasma gondii tachyzoites, bradyzoites, and sporozoites and biology and development of tissue cysts. Clin Microbiol Rev 1998, 11:267−299
3. Sims TA, Hay J, Talbot IC: An electron microscope and immuno-histochemical study of the intracellular location of Toxoplasma tissue cysts within the brains of mice with congenital toxoplasmosis. Br J Exp Pathol 1989, 70:317−325
4. Boothroyd JC, Black M, Bonnefoy S, Hehl A, Knoll LJ, Manger ID, Ortega-Barria E, Tomavo S: Genetic and biochemical analysis of development in Toxoplasma gondii. Philos Trans R Soc Lond B Biol Sci 1997, 352:1347−1354
5. Cong W, Liu GH, Meng QF, Dong W, Qin SY, Zhang FK, Zhang XY, Wang XY, Qian AD, Zhu XQ: Toxoplasma gondii infection in cancer patients: prevalence, risk factors, genotypes and association with clinical diagnosis. Cancer Lett 2015, 359:307−313
6. Thomas F, Lafferty KD, Brodeur J, Elguero E, Gauthier-Clerc M, Misse D: Incidence of adult brain cancers is higher in countries where the protozoan parasite Toxoplasma gondii is common. Biol Lett 2012, 8:101−103
7. Vittecoq M, Elguero E, Lafferty KD, Roche B, Brodeur J, Gauthier-Clerc M, Misse D, Thomas F: Brain cancer mortality rates increase with Toxoplasma gondii seroprevalence in France. Infect Genet Evol 2012, 12:496−498
8. Suzuki Y, Sa Q, Gehman M, Ochiai E: Interferon-gamma- and perforin-mediated immune responses for resistance against Toxoplasma gondii in the brain. Expert Rev Mol Med 2011, 13:e31
9. Munoz M, Liesenfeld O, Heimesaat MM: Immunology of Toxoplasma gondii. Immunol Rev 2011, 240:269−285
10. Suzuki Y, Wang X, Jortner BS, Payne L, Ni Y, Michie SA, Xu B, Kudo T, Perkins S: Removal of Toxoplasma gondii cysts from the brain by perforin-mediated activity of CD8$^+$ T cells. Am J Pathol 2010, 176:1607−1613
11. White DW, MacNeil A, Busch DH, Pilip IM, Pamer EG, Harty JT: Perforin-deficient CD8$^+$ T cells: in vivo priming and antigen-specific immunity against Listeria monocytogenes. J Immunol 1999, 162: 980−988
12. Kang H, Suzuki Y: Requirement of non-T cells that produce gamma interferon for prevention of reactivation of Toxoplasma gondii infection in the brain. Infect Immun 2001, 69:2920−2927
13. Suzuki Y, Orellana MA, Wong SY, Conley FK, Remington JS: Susceptibility to chronic infection with Toxoplasma gondii does not correlate with susceptibility to acute infection in mice. Infect Immun 1993, 61:2284−2288
14. Wang X, Claflin J, Kang H, Suzuki Y: Importance of CD8$^+$Vβ8$^+$ T cells in IFN-gamma-mediated prevention of toxoplasmic encephalitis in genetically resistant BALB/c mice. J Interferon Cytokine Res 2005, 25:338−344
15. Wang X, Kang H, Kikuchi T, Suzuki Y: Gamma interferon production, but not perforin-mediated cytolytic activity, of T cells is required for prevention of toxoplasmic encephalitis in BALB/c mice genetically resistant to the disease. Infect Immun 2004, 72: 4432−4438
16. Singh J, Graniello C, Ni Y, Payne L, Sa Q, Hester J, Shelton BJ, Suzuki Y: Toxoplasma IgG and IgA, but not IgM, antibody titers increase in sera of immunocompetent mice in association with proliferation of tachyzoites in the brain during the chronic stage of infection. Microbes Infect 2010, 12:1252−1257
17. Hester J, Mullins J, Sa Q, Payne L, Mercier C, Cesbron-Delauw MF, Suzuki Y: Toxoplasma gondii antigens recognized by IgG antibodies differ between mice with and without active proliferation of tachyzoites in the brain during the chronic stage of infection. Infect Immun 2012, 80:3611−3620
18. Wen X, Kudo T, Payne L, Wang X, Rodgers L, Suzuki Y: Predominant interferon-gamma-mediated expression of CXCL9, CXCL10, and CCL5 proteins in the brain during chronic infection with Toxoplasma gondii in BALB/c mice resistant to development of toxoplasmic encephalitis. J Interferon Cytokine Res 2010, 30: 653−660
19. Sa Q, Ochiai E, Tiwari A, Perkins S, Mullins J, Gehman M, Huckle W, Eyestone WH, Saunders TL, Shelton BJ, Suzuki Y: Cutting Edge: IFN-gamma produced by brain-resident cells is crucial to control cerebral infection with Toxoplasma gondii. J Immunol 2015, 195:796−800
20. Ochiai E, Sa Q, Brogli M, Kudo T, Wang X, Dubey JP, Suzuki Y: CXCL9 is important for recruiting immune T cells into the brain and inducing an accumulation of the T cells to the areas of tachyzoite proliferation to prevent reactivation of chronic cerebral infection with Toxoplasma gondii. Am J Pathol 2015, 185:314−324
21. Lan HY, Mu W, Nikolic-Paterson DJ, Atkins RC: A novel, simple, reliable, and sensitive method for multiple immunoenzyme staining: use of microwave oven heating to block antibody crossreactivity and retrieve antigens. J Histochem Cytochem 1995, 43:97−102
22. Nance JP, Vannella KM, Worth D, David C, Carter D, Noor S, Hubeau C, Fitz L, Lane TE, Wynn TA, Wilson EH: Chitinase dependent control of protozoan cyst burden in the brain. PLoS Pathog 2012, 8:e1002990
23. Sa Q, Ochiai E, Sengoku T, Wilson ME, Brogli M, Crutcher S, Michie SA, Xu B, Payne L, Wang X, Suzuki Y: VCAM-1/alpha4-beta1 integrin interaction is crucial for prompt recruitment of immune T cells into the brain during the early stage of reactivation of chronic infection with Toxoplasma gondii to prevent toxoplasmic encephalitis. Infect Immun 2014, 82:2826−2839
24. Ling YM, Shaw MH, Ayala C, Coppens I, Taylor GA, Ferguson DJ, Yap GS: Vacuolar and plasma membrane stripping and autophagic

elimination of Toxoplasma gondii in primed effector macrophages. J Exp Med 2006, 203:2063−2071

25. Selleck EM, Fentress SJ, Beatty WL, Degrandi D, Pfeffer K, Virgin HWt, Macmicking JD, Sibley LD: Guanylate-binding protein 1 (Gbp1) contributes to cell-autonomous immunity against Toxoplasma gondii. PLoS Pathog 2013, 9:e1003320

26. Divanovic S, Sawtell NM, Trompette A, Warning JI, Dias A, Cooper AM, Yap GS, Arditi M, Shimada K, Duhadaway JB, Prendergast GC, Basaraba RJ, Mellor AL, Munn DH, Aliberti J, Karp CL: Opposing biological functions of tryptophan catabolizing enzymes during intracellular infection. J Infect Dis 2012, 205:152−161

27. Suzuki Y, Joh K, Orellana MA, Conley FK, Remington JS: A gene(s) within the H-2D region determines the development of toxoplasmic encephalitis in mice. Immunology 1991, 74:732−739

28. Brown CR, McLeod R: Class I MHC genes and CD8^{+} T cells determine cyst number in Toxoplasma gondii infection. J Immunol 1990, 145:3438−3441

29. Ferguson DJ, Hutchison WM: An ultrastructural study of the early development and tissue cyst formation of Toxoplasma gondii in the brains of mice. Parasitol Res 1987, 73:483−491

30. Ghatak NR, Zimmerman HM: Fine structure of Toxoplasma in the human brain. Arch Pathol 1973, 95:276−283

31. Sa Q, Ochiai E, Tiwari A, Mullins J, Shastri N, Mercier C, Cesbron-Delauw MF, Suzuki Y: Determination of a key antigen for immunological intervention to target the latent stage of Toxoplasma gondii. J Immunol 2017, 198:4425−4434

32. Sullivan WJ Jr, Jeffers V: Mechanisms of Toxoplasma gondii persistence and latency. FEMS Microbiol Rev 2012, 36:717−733

33. Suss-Toby E, Zimmerberg J, Ward GE: Toxoplasma invasion: the parasitophorous vacuole is formed from host cell plasma membrane and pinches off via a fission pore. Proc Natl Acad Sci U S A 1996, 93:8413−8418

34. Wensink AC, Hack CE, Bovenschen N: Granzymes regulate proinflammatory cytokine responses. J Immunol 2015, 194:491−497

35. Sa Q, Tiwari A, Ochiai E, Mullins J, Suzuki Y: Inducible nitric oxide synthase in innate immune cells is important for restricting cyst formation of Toxoplasma gondii in the brain but not required for the protective immune process to remove the cysts. Microbes Infect 2018, 20:261−266

36. Masson F, Calzascia T, Di Berardino-Besson W, de Tribolet N, Dietrich PY, Walker PR: Brain microenvironment promotes the final functional maturation of tumor-specific effector CD8^{+} T cells. J Immunol 2007, 179:845−853

37. Huang LR, Wohlleber D, Reisinger F, Jenne CN, Cheng RL, Abdullah Z, Schildberg FA, Odenthal M, Dienes HP, van Rooijen N, Schmitt E, Garbi N, Croft M, Kurts C, Kubes P, Protzer U, Heikenwalder M, Knolle PA: Intrahepatic myeloid-cell aggregates enable local proliferation of CD8^{+} T cells and successful immunotherapy against chronic viral liver infection. Nat Immunol 2013, 14:574−583

38. Wilson EH, Harris TH, Mrass P, John B, Tait ED, Wu GF, Pepper M, Wherry EJ, Dzierzinski F, Roos D, Haydon PG, Laufer TM, Weninger W, Hunter CA: Behavior of parasite-specific effector CD8^{+} T cells in the brain and visualization of a kinesis-associated system of reticular fibers. Immunity 2009, 30:300−311

39. Schaeffer M, Han SJ, Chtanova T, van Dooren GG, Herzmark P, Chen Y, Roysam B, Striepen B, Robey EA: Dynamic imaging of T cell-parasite interactions in the brains of mice chronically infected with Toxoplasma gondii. J Immunol 2009, 182:6379−6393

40. Finn OJ: A believer's overview of cancer immunosurveillance and immunotherapy. J Immunol 2018, 200:385−391